

PAPER

View Article Online  
View Journal | View Issue



Cite this: *Environ. Sci.: Nano*, 2024, 11, 812

# Europium-doped layered double hydroxide with spectral conversion property for enhanced photosynthesis†

Chong Wang,<sup>a</sup> Zixian Li,<sup>b</sup> Yufei Zhao,<sup>b</sup> Changjiao Sun,<sup>a</sup> Yue Shen,<sup>a</sup> Shenshan Zhan,<sup>a</sup> Xingye Li,<sup>a</sup> Qi Liu,<sup>a</sup> Weichang Gao,<sup>c</sup> Tao Li<sup>a</sup> and Yan Wang<sup>\*a</sup>

Photosynthesis paves a sustainable way to meet the growing demand for food and agricultural products. Herein, a europium-doped layered double hydroxide (Eu-LDH) architecture was designed via a co-precipitation method to augment photosynthesis. DFT calculations and characterization data revealed that the doped Eu atoms bestow the architecture with photo-responsive properties through the regulation of the density of states and the optimization of the bandgap structure. Eu-LDH possesses the spectral conversion effect that converts the poorly utilized UV light into the strongly absorbed red light in plants. By the scientific and accurate foliar spraying, Eu-LDH demonstrated an enhanced photosynthetic efficiency in *Nicotiana benthamiana*, improving the photosynthetic rate, leaf area, fresh weight, and dry weight by 15.1%, 34.3%, 35.7%, and 16.7%, respectively. Moreover, the interaction between Eu-LDH and plant leaves was put forward as a key factor that is responsible for the promotion of photosynthesis. It ensured the duration of Eu-LDH on the leaf surface and provided an appropriate light environment for plants to carry out photosynthesis. These findings deepen the understanding of spectral conversion based on Eu-LDH with the engineered band gap structure towards increasing production and sustainable agricultural development.

Received 16th June 2023,  
Accepted 18th December 2023

DOI: 10.1039/d3en00394a

rs.li/es-nano

## Environmental significance

Photosynthesis is an essential and complex process that converts solar energy into chemical energy in plants. It is the source of most food and agricultural supply all over the world. In this work, a europium doped layered double hydroxides (Eu-LDH) architecture is designed via a co-precipitation method to augment photosynthesis. Revealed by DFT calculations and characterization, the doped Eu atoms bestow the architecture with photo-responsive properties via the regulation of the density of states and the bandgap structure. Eu-LDH possesses the spectral conversion effect that converts the poorly utilized UV light into the strongly absorbed red light. The optimized propagation symmetry of light provided extra photons to participate in photosynthesis and to achieve enhanced photosynthetic efficiency, leaves area, and biomass accumulation on *Nicotiana benthamiana*. Moreover, the interaction between Eu-LDH and plant leaves is forward as a key factor that is responsible for the promoted photosynthesis. It ensured the duration of Eu-LDH on the surface of leaves and provided the appropriate light environment for plants to carry out photosynthesis. These findings deepen the understanding of spectral conversion based on Eu-LDH with the engineered band gap structure for increasing production and sustainable agricultural development.

## 1. Introduction

Photosynthesis is an essential and complex process involving the conversion of solar energy into chemical energy in plants.<sup>1</sup> It is the source of most food and agricultural supplies worldwide. However, not every spectral component of sunlight equally contributes to photosynthesis. The blue (400–500 nm) and red (600–700 nm) portions are strongly

absorbed by chlorophyll, while the green light (500–600 nm) is mostly reflected.<sup>2</sup> Generally, less than 10% of sunlight meets the need for photosynthesis, which severely limits the improvement of photosynthetic efficiency.

In order to overcome this limitation to meet the growing food demand of over 8 billion people all over the world, light-harvesting nanomaterials, such as carbon dots (CDs),<sup>3</sup> semiconductors quantum dots, (QDs),<sup>4</sup> fluorescent polymers, and rare earth materials, have been employed to broaden the available spectral range by the conversion of poorly absorbed ultraviolet (UV) or/and green light to highly absorbed red or/and blue light to boost photosynthesis.<sup>5</sup> Although much efforts have been taken, the efficiency of spectral conversion is still not satisfactory. Except for the intrinsic reasons, including photostability and quantum efficiency, the roll

<sup>a</sup> Institute of Environment and Sustainable Development in Agriculture, Chinese Academy of Agricultural Sciences, Beijing, 100081, China. E-mail: wangyang03@caas.cn

<sup>b</sup> Beijing University of Chemical Technology, P. R. China, Beijing, 100081, China

<sup>c</sup> Guizhou Academy of Tobacco Science, Upland Flue-cured Tobacco Quality & Ecology Key Laboratory of CNTC, Guiyang, 550081, P. R. China

† Electronic supplementary information (ESI) available. See DOI: <https://doi.org/10.1039/d3en00394a>



down of light conversion materials from plant leaves during the spraying application is also a key barrier. It leads to a loss of active ingredients from more than 90% of plant leaves.<sup>6</sup> Therefore, for a well-designed spectral conversion material, the foliar adhesion behavior and the spectral conversion performance should be treated as critical factors.

Layered double hydroxide (LDH) is a typical inorganic lamellar material with abundant hydroxyl groups. It is generally expressed by the following formula:

$$[M^{2+}_{(1-x)}M^{3+}_x(OH)_2] \cdot (A^{n-})_{x/n} \cdot mH_2O$$

in which,  $M^{2+}$ ,  $M^{3+}$ , and  $A^{n-}$  are divalent and trivalent metals and interlayered anions, respectively.<sup>7</sup> Owing to the diversity of metal ions in the laminate structure, the electronic structure and energy band of LDH can be easily optimized *via* the regulation of metal composition and the doping of rare earth elements.<sup>8,9</sup> It leads to improved performance in the fields of photocatalysis and electrochemistry through the transformation of hydroxides into oxides,<sup>10</sup> nitrides, or metals.<sup>11</sup> Although the hydroxide structure has no obvious advantage in the field of photocatalysis and electrocatalysis, the rich hydroxyl groups have illustrated a satisfactory carrier effect in the application of nano-pesticide in our reported work.<sup>12</sup> The hydrogen bonds between the surface groups of the plant leaves such as carboxyl and hydroxyl groups and LDH enhance the foliar adhesion rate and reduce the loss of active ingredients.<sup>13</sup> Therefore, the construction of LDH with foliar adhesion and elaborate electronic structure represents a promising strategy to promote efficient and lasting photosynthesis by spectral conversion.

In this work, the europium-doped layered double hydroxide (Eu-LDH) architecture was designed using a coprecipitation method. As confirmed by the computational simulation and characterization, Eu-LDH showed spectral conversion performance through the doping of Eu atoms into the Eu-LDH crystal structure. The replacement of Eu atoms for Al atoms show a substantial contribution to the electronic structure of Eu-LDH and narrow the bandgap from ~3.82 to ~3.07 eV. It endows the Eu-LDH architecture with photo-responsive characteristics within a suitable wavelength range and provides the possibility to achieve spectral conversion. The scientific and accurate foliar spraying on *Nicotiana benthamiana*, enhanced the photosynthetic efficiency of leaves area, leaf fresh weight, and biomass accumulation by 15.1%, 34.3%, 35.7%, and 16.7%, respectively. The mechanism was clarified through the spectral conversion from the poorly utilized UV light (~390 nm) to strongly absorbed red light (~610 and 700 nm) (Fig. 1). The optimized propagation symmetry of light provided a suitable local light environment for plants with extra photons participating in photosynthesis. It induces an enhanced photosynthetic rate and more biomass accumulation. Moreover, the hydrogen bonds between Eu-LDH and plant leaves were put forward as key factors responsible for the promoted photosynthesis. It ensured the duration of the appropriate light environment

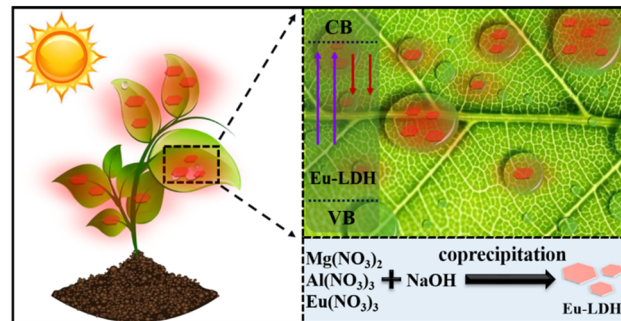


Fig. 1 Schematic illustration of the spectral conversion of Eu-LDH on a leaf.

for leaves to carry out photosynthesis. Therefore, this study provides the Eu-LDH architecture and related mechanisms to achieve more biomass accumulation by enhanced photosynthetic efficiency. It represents the immense promising method to introduce nano-materials into agricultural production to realize sustainable development.

## 2. Experimental section

### 2.1. Reagent and characterization

$Mg(NO_3)_2 \cdot 6H_2O$ ,  $Al(NO_3)_3 \cdot 9H_2O$ ,  $Eu(NO_3)_3 \cdot 6H_2O$ , and NaOH were purchased from Beijing Chemical Works (Beijing, China). All the chemicals were analytical reagent grade and used without further purification. Two commercially available photosynthesis-enhancing agents with the effective components of triacontanol and gibberellic acid were purchased from Sichuan Guoguang Agrochemical Co., Ltd. and Zhejiang Biok Biological Technology Co., Ltd., respectively.

Powder X-ray diffraction patterns were collected using a Bruker D8 Advance X-ray diffractometer using a Cu K $\alpha$  source, at a scan rate of 10° min<sup>-1</sup>. The concentration of Eu was measured using an inductively coupled plasma optical emission spectrometer (ICP-OES, Agilent ICPOES730). X-ray photoelectron spectroscopy (XPS) measurements were performed on ESCALAB 250Xi Thermo Scientific with Al K $\alpha$  radiation. Binding energies were determined with adventitious carbon (C1s at 284.6 eV) as the reference. The morphology of the samples was investigated using a scanning electron microscope (SEM; Zeiss SUPRA 55) with an accelerating voltage of 20 kV. High-resolution transmission electron microscopy (HR-TEM) images were recorded with JEOL JEM-2010 equipment with an accelerating voltage of 200 kV. The UV-vis absorption and emission spectra were recorded on a fluorescence spectrometer, FL1000/FS5, Edinburgh Instruments Ltd, UK. The contact angle pictures were collected on the contact angle (CA) instrument with an automatic microinjector (JC2000D2M, Zhongchen Digital Technic Apparatus Company, Ltd., China). Every measurement was repeated at least five times.

### 2.2. Synthesis of Eu-LDH

$Mg(NO_3)_2 \cdot 6H_2O$  (0.1 M),  $Al(NO_3)_3 \cdot 9H_2O$  (0.045 M) and  $Eu(NO_3)_3 \cdot 6H_2O$  (0.005 M) were dissolved in deionized water



(200 mL) as solution A. NaOH (0.3 M) was dissolved in another 200 mL deionized water to obtain solution B. Afterwards, the two solutions were mixed by vigorous stirring (3000 rpm) with colloid mill for 3 min. The resulting solution was centrifuged at 10 000 rpm for 10 min and washed several times with ethanol and deionized water. Until the supernatant was neutral, the Eu-LDH nanosheets were collected for further use.

### 2.3. Calculation method

The calculations in this work were performed using the CASTEP code in the Materials Studio (version 8.0) software package (Accelrys Software Inc., San Diego, CA).<sup>14</sup> The spin-polarized DFT+U calculations were performed through a plane wave implementation<sup>15</sup> with the generalized gradient approximation (GGA) Perdew–Burke–Ernzerhof (PBE) as the exchange-correlation functional.<sup>16</sup> More parameters and corrections were detailed in the ESI.†

### 2.4. Plant cultivation

For the cultivation, the seeds were disinfected with 1% NaClO aqueous solution for 15 min. After washing 3 times with deionized water and drying in air, the seeds were placed on a germination tray at 30 °C. Then, the germinated seedlings were transplanted into the pots (10 × 10 × 10 cm). 5 plants were set for a treatment; every treatment was repeated 3 times. After 7 days, the Eu-LDH aqueous solution (1.0 g L<sup>-1</sup>) was sprayed on leaves. The spraying treatment was repeated every 3 days, with 3 times in total. Two weeks after the spraying treatment, the growth parameters and photosynthesis rates were recorded. The photosynthesis rate was measured using the LI-6800 photosynthetic system under the photon flux density (Q) of 200 μmol m<sup>-2</sup> s<sup>-1</sup> (LI-COR, Inc., America.). The Hoagland nutrient solution was used during the cultivation process.

### 2.5. Statistical analysis

All data in this work are presented as mean ± standard deviation (SD), obtained using the IBM SPSS 20.0 software. Statistical significance was determined using the one-way analysis of variance (one-ANOVA), followed by the Duncan test. Samples having *p*-values < 0.05 showed a significant difference. The \* represents a significant difference.

## 3. Results and discussion

### 3.1. Morphology and chemical structure of Eu-LDH

Fig. 2A shows the X-ray diffraction (XRD) pattern of Eu-LDH (blue line). The diffraction peaks at 10.01°, 20.13°, 33.45°, and 59.54° are indexed to (003), (006), (012), and (110) reflection peaks of the LDH phase with the NO<sub>3</sub><sup>-</sup> ions interlayered in the gallery. The commercially available LDH sample (MgAl-LDH, J&K Scientific, 99%) was employed as a reference (orange line). According to the comparison of the strongest (003) diffraction peak intensity, the crystallinity was

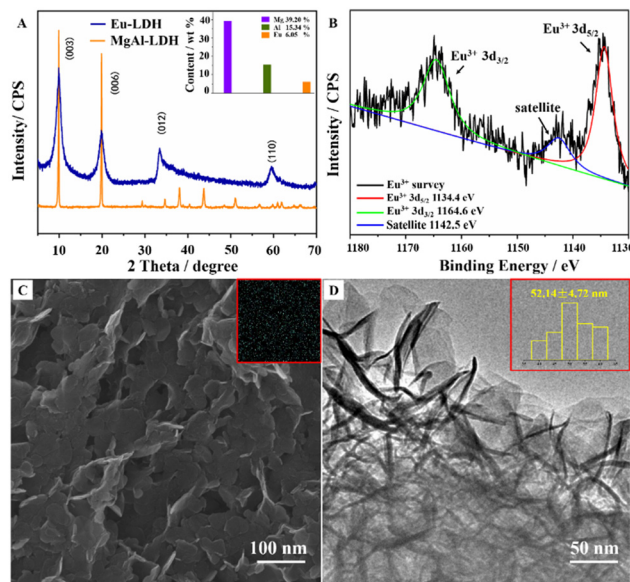


**Fig. 2** (A) XRD patterns of Eu-LDH (blue line) and MgAl-LDH reference (orange line). Inset of the metal element content by ICP-AES. (B) The XPS spectrum of Eu in Eu-LDH. (C) SEM image of Eu-LDH. Inset for the EDS analysis of Eu element. (D) HR-TEM image of Eu-LDH. Inset for the size distribution of Eu-LDH.

estimated to be ~80%. The metal element contents were confirmed by ICP-AES and shown in the inset. It demonstrated that the LDH structure was doped by the Eu element with high crystallinity.

The Eu element can form the laminate structure in the state of Eu<sup>2+</sup> and Eu<sup>3+</sup> with different excited luminescence. X-ray photoelectron spectroscopy (XPS) was employed to elucidate the valence states of the Eu element in Eu-LDH. As shown in Fig. 2B, the Eu spectrum can be deconvoluted into three peaks, including 1164.6 eV for Eu<sup>3+</sup> 3d<sub>5/2</sub> (green line), 1142.5 eV for satellite (blue line) and 1134.4 eV for Eu<sup>3+</sup> 3d<sub>5/2</sub> (red line) peaks.<sup>17</sup> It confirms that all the Eu species in the Eu-LDH structure exist in trivalent ions. The morphology of Eu-LDH was observed using the scanning electron microscope (SEM) and high-resolution transmission electron microscope (HR-TEM). As shown in Fig. 2C and D, Eu-LDH possesses a sheet-like hexagon nanoplate morphology with a mean particle size of ~50 nm. The Eu-LDH was further characterized by EDS analysis and shown in the Fig. 4C inset, from which it was observed that the Eu element was homogeneously distributed throughout the architecture.

### 3.2. Study on the structure and optical property correlation of Eu-LDH

To investigate the mechanism underlying the spectral conversion, the spin-polarized density functional theory (DFT) calculation was carried out to give a deep insight into the influence on the electronic structure of the Eu-LDH. The parameters and corrections are detailed in the ESI.† As shown in Fig. 3A and B, the models of MgAl-LDH and Eu-LDH were





built with the unit cell set as  $5 \times 6 \times 1$ . The partial Al atoms were replaced with Eu atoms to define the Eu-LDH structure in order to keep consistent with the characterization in the experiment. Accordingly, the density of states (DOS) of MgAl-LDH and Eu-LDH were calculated to reveal the relationship between the electronic structure and optical effect. From the total density of states (T-DOS) of Eu-LDH and MgAl-LDH, as shown in Fig. 3C and D, it can be observed that the T-DOS of Eu-LDH comprises P-DOS of O, Eu, Mg, and Al, while the T-DOS of MgAl-LDH comprises P-DOS of O, Mg, and Al. In the two architectures. Due to the substantial contribution of Eu atoms to the T-DOS (blue line in Fig. 3C), the doping of Eu atoms shows an obvious influence on the electronic structure of Eu-LDH. Compared with that of MgAl-LDH, the doping of trivalent Eu atoms narrows the bandgap from  $\sim 3.82$  to  $\sim 3.07$  eV. It endows the Eu-LDH architecture with photo-responsive characteristics within a suitable wavelength range and provides the possibility to achieve spectral conversion. To confirm the computational simulation, the optical characterization of the Eu-LDH was carried out to measure the photo-responsive property. As shown in Fig. 3E and F, the UV-vis absorption spectrum of the Eu-LDH sample exhibits a series of peaks at 362 nm, 376 nm, 380 nm, 394 nm, and 464 nm, which are attributed to the electronic transitions of  ${}^7F_0 \rightarrow {}^5D_4$ ,  ${}^7F_0 \rightarrow {}^5D_3$ ,  ${}^7F_0 \rightarrow {}^5D_3$ ,  ${}^7F_0 \rightarrow {}^5D_3$ , and  ${}^7F_0 \rightarrow {}^5D_2$ , respectively. The 394 nm is selected as the excitation wavelength in the photoluminescence spectrum of Eu-LDH. In the excited spectrum, the peaks are attributed to the electronic de-excitation from the  ${}^5D_0$  level to the  ${}^7F_J = 0-4$  ground state.<sup>18</sup> Under excitation, it showed red emission light with a mixed wavelength of 610 and 700 nm. The digital image of Eu-LDH powder is shown as the inset in Fig. 3F. Moreover, the maximum absorption wavelength of 394 nm was employed to calculate the theoretical band gap according to the equation:

$$E = h\nu = hc/\lambda$$

in which,  $E$  (eV) represents the absorbed photon energy;  $\nu$  represents photon frequency (Hz);  $\lambda$  represents the photon wavelength (m);  $h$  is the Planck constant ( $6.62607015 \times 10^{-34}$  J s or  $4.1356676969 \times 10^{-15}$  eV s);  $c$  is the speed of light in vacuum ( $2.99792458 \times 10^8$  m s $^{-1}$ ). The band gap of Eu-LDH calculated by this method was  $\sim 3.15$  eV, which matches well with that obtained from DFT calculations. Besides, the excitation wavelength of Eu-LDH after aging for 100 h in an ultraviolet-accelerated weatherometer was also investigated. As the T-DOS consists of O, Eu Mg, and Al atoms in metal-oxygen (M-O) bonds with UV stability, the Eu-LDH structure shows stable light response characteristics. After aging for 100 h, it still possesses the spectral conversion effect with the quantum efficiency decreasing from 9.2% to 7.8%. The photoluminescence spectra of Eu-LDH before and after aging for 100 h by ultraviolet accelerated weatherometer and the quantum efficiency are shown in the ESI,† Fig. S1. Therefore, as revealed by DFT calculations and characterization, such an

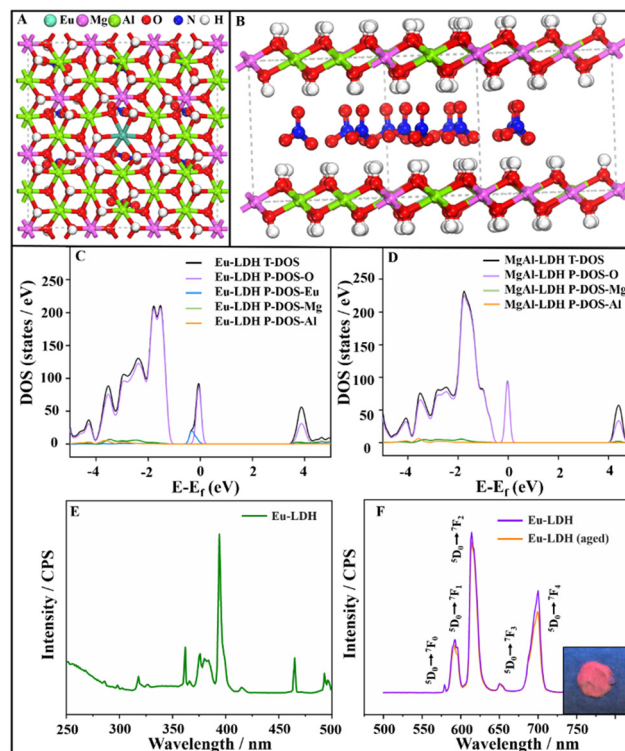


Fig. 3 (A) Schematic illustration and (B) side view of the Eu-LDH structure. The total density of states of (C) Eu-LDH and (D) MgAl-LDH. (E) UV-vis absorption and (F) photoluminescence spectrum of Eu-LDH. Inset for the image of powder Eu-LDH under excitation.

Eu-LDH structure possesses the spectral conversion ability, accounting for the optimization of the plant's favourable light environment.

### 3.3. Measurement of foliage surface behavior of Eu-LDH

As the Eu-LDH was designed for the spraying application, the foliage surface behaviors of Eu-LDH including wettability and retention rate were investigated to measure the sustainability of the optimized light environment on leaves against rolling down. The wettability of Eu-LDH was operated on *Nicotiana benthamiana* leaves. It was reflected in the contact angle (CA) with the Eu-LDH concentration of  $1.0 \text{ g L}^{-1}$ . As shown in Fig. 4A and B, the CA of Eu-LDH reached  $\sim 27.6^\circ$ , while the CA of water reached  $\sim 78.4^\circ$ . The infiltration effect was attributed to the existence of rich hydroxyl groups on the LDH. They can form hydrogen bonds with the polar groups on the foliage surface, which results in the quick spreading of Eu-LDH drops on leaves and overcomes the hydrophobic interaction of the surface wax and villi structure. Taking advantage of the fluorescent characteristic of Eu-LDH, the variation ( $R\%$ ) of fluorescence intensity before ( $I_0$ ) and after ( $I$ ) washing was investigated to calculate the retention rate ( $I/I_0$ ) to measure the foliage adhesion based on the reported method.<sup>19</sup> Accordingly, the Eu-LDH solution was uniformly sprayed onto the surface of the leaf. After drying in air at room temperature, the treated leaf sample was subjected to



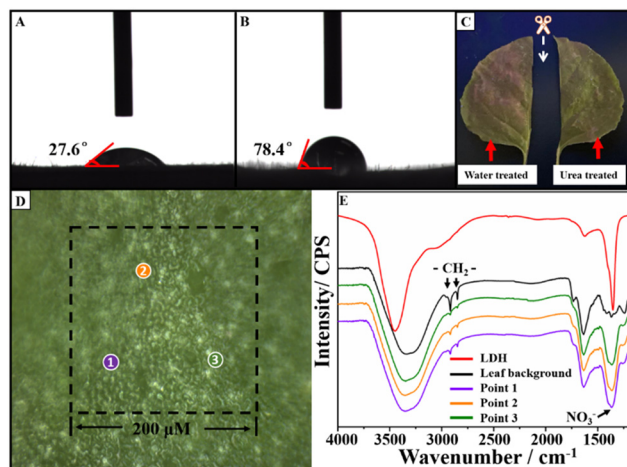


Fig. 4 Measurement of foliage surface behavior. Contact angle images on a leaf of (A) Eu-LDH solution and (B) water. (C) Fluorescent image of two half leaves washed with water and 5% urea solution. (D) Image of the selected areas on the leaf and (E) FT-IR spectra at randomly selected points with LDH and leaf background as references.

LSCM (LSM 710, Carl Zeiss, Germany) at the excitation wavelength and captured by an imaging system. Afterwards, the leaf was then cut into two halves, one half was washed with 100 mL of deionized water to simulate the washout by rain, while the other half was washed with 100 mL 5% urea solution as the hydrogen bonds destroying agent. The two half-leaf samples were subjected to LSCM again. Then, the fluorescence intensity before ( $I_0$ ) and after ( $I$ ) washing can be integral simulation calculated using the software (Zeiss Zen 3.4). As shown in Fig. 4C, after washing with water and urea solution, the retention rates reached 61.73% and 22.45%, respectively. The results showed that the Eu-LDH maintained a good adhesion rate under the wash by water, but it can be easily washed off by urea solution. The difference indicated that urea molecules destroyed the key interaction of hydrogen bonds, which is consistent with the mentioned foliar adhesion mechanism. Moreover, FTIR microscopy was employed to confirm the existence of Eu-LDH on the leaves' surface. As shown in Fig. 4D and E, the infrared spectra at 3 randomly selected points were collected. For the background infrared spectrum of the leaf surface (black line), the characteristic absorption peaks at 2971 and 2851  $\text{cm}^{-1}$  are attributed to the asymmetric and symmetric stretching vibrations of the  $-\text{CH}_2-$  structure on the leaf surface, respectively. Compared with that, the spectra of the selected points showed the characteristic absorption peak of the  $\text{NO}_3^-$  group in Eu-LDH at  $\sim 1370 \text{ cm}^{-1}$ , which illustrated the uniform and stable distribution of Eu-LDH on the leaf surface. The results demonstrated the advantage of Eu-LDH in the wettability and adhesion effect. Benefitting from the existence of rich hydroxyl groups, Eu-LDH possesses improved spreading and retention properties on leaves, and effectively avoids the droplet rolling caused by the hydrophobic structure. It provides the possibility to optimize the local light environment and ensures effective duration.

### 3.4. Effect of Eu-LDH on the photosynthesis and growth

The role of Eu-LDH in the regulation of photosynthesis and growth was evaluated by the scientific and appropriate foliar application on *Nicotiana benthamiana*. The samples treated by water (CK group), LDH, and mixed nitrate solution ( $\text{Mg}(\text{NO}_3)_2$ ,  $\text{Al}(\text{NO}_3)_3$ ,  $\text{Eu}(\text{NO}_3)_3$ ) with the same concentration in Eu-LDH were employed as references. As shown in Fig. 5, the samples of LDH and mixed nitrate solution showed no differences in the plant growth with the CK sample, but the sample treated by Eu-LDH exhibited a 15.1% increase in the photosynthetic rate with a significant difference. Furthermore, for the representative physiological indexes including leaf area, fresh leaves weight, and dry matter accumulation, the Eu-LDH group also achieved increases of 34.3%, 35.7%, and 16.7%, respectively. For the reference samples, the photosynthetic rate and physiological indexes showed no obvious differences compared with the CK group.

The representative growth state images are shown in Fig. 5E and F, except for the larger plant shape, the flower bud formation time was also investigated. The results are given in Fig. 5F. It can be observed that the application of Eu-LDH promoted flower bud formation with substantial differences. By the formation of flower buds, plants start reproductive growth and enter the ripening process. It directly affects the yield and quality of plants. Therefore, this method may hold the possibility to promote the early maturity of crops, shorten the cultivation cycle, and increase economic value. The individual images of Eu-LDH treated seedlings and the flower bud formation time information are given in the ESI,† Fig. S2 and Table S1.

Two commercially available photosynthesis-enhancing agents with the effective components of triacontanol (Sichuan Guoguang Agrochemical Co., Ltd.) and gibberellic acid (GA3, Zhejiang Biok Biological Technology Co., Ltd) were measured as the references samples. They were labelled as Tria and GA, respectively. As shown in Fig. 6, all the samples showed obvious effects on leaf areas. Additionally, the Tria

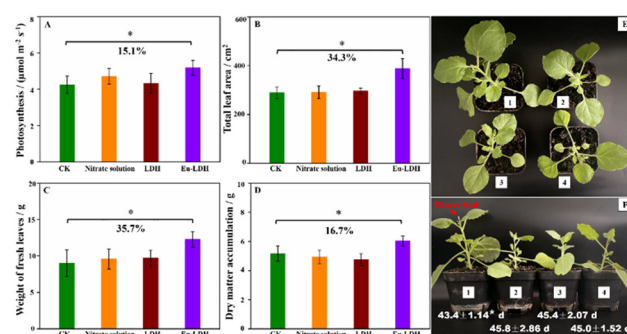


Fig. 5 Physiological indices of *Nicotiana benthamiana* with different treatment groups. (A) Photosynthetic rate; (B) total leaf area; (C) weight of fresh leaves and (D) dry matter accumulation. (E) Top and (F) side view photographs of different treated plants with the order of 1. Eu-LDH; 2. mixed nitrate solution; 3. LDH and 4. CK samples. The flower bud formation time was marked in the figure. The \* represents the significant difference compared with CK ( $P < 0.05$ ).



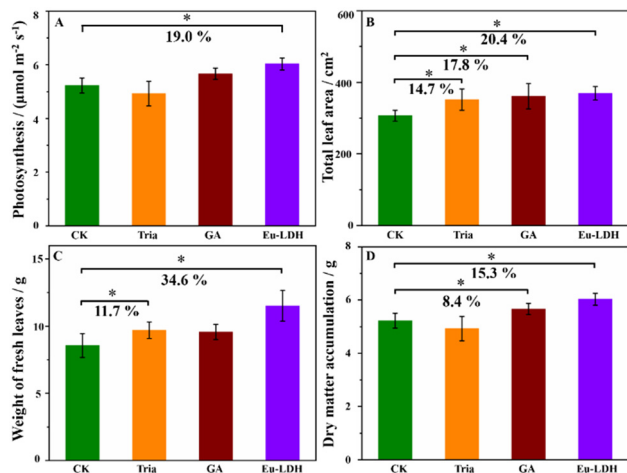


Fig. 6 The physiological indices of *Nicotiana benthamiana* with different commercially available photosynthesis-enhancing agents treatment groups. (A) Photosynthetic rate; (B) total leaf area; (C) weight of fresh leaves and (D) dry matter accumulation. \* represents the significant difference compared with CK ( $P < 0.05$ ).

treatment promoted the weight of fresh leaves by 11.7%, while the GA treatment increased the dry weight accumulation by 8.4%. However the Tria and GA treatments showed little impact on the photosynthesis rate. For the Eu-LDH treatment, it showed comprehensive advantages in the mentioned physiological indexes.

These results can be summarized that the application of Eu-LDH optimized the propagation symmetry of light and provided the local light environment with extra photons to participate in the photosynthesis process. Then, the plants with the favourable growth situation and larger leaf areas accepted more photons. Under the adequate nutrient supply, this positive feedback resulted in more fresh leaves weight, dry matter accumulation, and better maturity. Therefore, these findings clarified that the existence of  $\text{Eu}^{3+}$  ions or the LDH structure without the suitable bandgap structure does not affect plant photosynthesis, only through the construction of a photo-responsive bandgap structure can we gain the property to promote plant growth by spectral conversion.

## 4. Conclusions

In summary, the Eu-LDH architecture was designed *via* a co-precipitation method and explored as a spectral conversion material for improved photosynthetic efficiency with enhanced foliar adhesion and prolonged duration. Benefiting from the doping of Eu atoms in the laminate structure, the Eu-LDH achieved band structure optimization and obtained the photo-responsive property. It can convert poorly utilized light to strongly absorbed red light, which improves the local light environment for plant growth. Taking the comprehensive advantages of the spectral conversion effect and enhanced foliar adhesion, the application of Eu-LDH achieved the improvement in photosynthetic rate, leaves area, fresh weight, and dry weight accumulation of 15.1%, 34.3%,

35.7%, and 16.7% on *Nicotiana benthamiana*, respectively. It also promotes the flower bud formation and holds the possibility to promote the early maturity of crops. Therefore, this study suggests a promising method to obtain enhanced photosynthesis and agricultural products by the optimized optical propagation with the application of Eu-LDH.

## Author contributions

C. Wang, T. Li, and Y. Wang designed the research; C. Wang, C. Sun, and S. Zhan performed the experiment; Z. Li and Y. Zhao supported the computational investigation and analysis; Y. Shen and X. Li performed the measurement of foliar behaviors; Q. Liu and W. Gao supervised the characterization of infrared microscope and the cultivation of plants; T. Li supervised the photosynthesis experiment; C. Wang wrote the paper. T. Li, and Y. Wang proofread and commented on the manuscript.

## Conflicts of interest

The authors declare no competing financial interest.

## Acknowledgements

This work was supported by the Young Scientists Fund of the National Natural Science Foundation of China (No. 22208372), the National Key R&D Program of China (2021YFA0716704), and the Key Program for Science and Technology of CNTC (110202202030).

## Notes and references

- 1 T. B. Arp, J. Kistner-Morris, V. Aji, R. J. Cogdell, R. V. Grondelle and N. M. Gabor, Quieting a noisy antenna reproduces photosynthetic light-harvesting spectra, *Science*, 2020, **368**, 1490.
- 2 M. D. Ooms, C. T. Dinh, E. H. Sargent and D. Sinton, Photon management for augmented photosynthesis, *Nat. Commun.*, 2016, **7**, 12699.
- 3 Y. Li, X. Pan, X. Xu, Y. Wu, J. Zhuang, X. Zhang, H. Zhang, B. Lei, C. Hu and Y. Liu, Carbon dots as light converter for plant photosynthesis: Augmenting light coverage and quantum yield effect, *J. Hazard. Mater.*, 2021, **410**, 124534.
- 4 X. Zhou, Y. Zeng, F. Lv, H. Bai and S. Wang, Organic Semiconductor–Organism Interfaces for Augmenting Natural and Artificial Photosynthesis, *Acc. Chem. Res.*, 2022, **55**, 156.
- 5 G. Pennisi and F. Orsini, Increasing greenhouse production by spectralshifting and unidirectional light-extracting photonics, *Nat. Food*, 2021, **2**, 394.
- 6 X. Zhao, H. Cui, Y. Wang, C. Sun, B. Cui and Z. Zeng, Development strategies and prospects of nano-based smart pesticide formulation, *J. Agric. Food Chem.*, 2018, **66**, 6504.
- 7 T. Hu, Z. Gu, G. R. Williams, M. Strimaite, J. Zha, Z. Zhou, X. Zhang, C. Tan and R. Liang, Layered double hydroxide-based nanomaterials for biomedical applications, *Chem. Soc. Rev.*, 2022, **51**, 6126.





- 8 T. Hu, L. Yan, Z. Wang, W. Shen, R. Liang, D. Yan and M. Wei, A pH-responsive ultrathin Cu-based nanopatform for specific photothermal and chemodynamic synergistic therapy, *Chem. Sci.*, 2021, **12**, 2594.
- 9 Y. Fu, F. Ning, S. Xu, H. An, M. Shao and M. Wei, Terbium doped ZnCr-layered double hydroxides with largely enhanced visible light photocatalytic performance, *J. Mater. Chem. A*, 2016, **4**, 3907.
- 10 Y. Zhao, X. Jia, G. Chen, L. Shang, G. I. N. Waterhouse, L.-Z. Wu, C.-H. Tung, D. O'Hare and T. Zhang, Ultrafine NiO nanosheets stabilized by TiO<sub>2</sub> from monolayer NiTi-LDH precursors: An active water oxidation electrocatalyst, *J. Am. Chem. Soc.*, 2016, **138**, 6517.
- 11 F. Song and X. Hu, Exfoliation of layered double hydroxides for enhanced oxygen evolution catalysis, *Nat. Commun.*, 2014, **5**, 4477.
- 12 C. Wang, F. Gao, C. Sun, Y. Shen, S. Zhan, X. Li, H. Cui, L. Duan, Y. Wang and Y. Wang, Self-assembly of 1-triacontanol onto layered doubled hydroxide nano-carriers toward sustainable growth regulation of maize, *Environ. Sci.: Nano*, 2022, **9**, 797.
- 13 H. Zhi, H. Chen, M. Yu, C. Wang, B. Cui, X. Zhao, Y. Wang, H. Cui, B. Zhang and Z. Zeng, Layered Double Hydroxide nanosheets improve the adhesion of fungicides to leaves and the antifungal performance, *ACS Appl. Nano Mater.*, 2022, **5**, 5316.
- 14 M. D. Segall, J. D. L. Philip, M. J. Probert, C. J. Pickard, P. J. Hasnip, S. J. Clark and M. C. Payne, First-principles simulation: ideas, illustrations and the CASTEP code, *J. Phys.: Condens. Matter*, 2002, **14**, 2717.
- 15 M. C. Payne, M. P. Teter, D. C. Allan, T. A. Arias and J. D. Joannopoulos, Iterative minimization techniques for *ab initio* total-energy calculations: molecular dynamics and conjugate gradients, *Rev. Mod. Phys.*, 1992, **64**, 1045.
- 16 J. P. Perdew, K. Burke and M. Ernzerhof, Generalized gradient approximation made simple, *Phys. Rev. Lett.*, 1996, **77**, 3865.
- 17 L. Wang, H. Zhou, J. Hu, B. Huang, M. Sun, B. Dong, G. Zheng, Y. Huang, Y. Chen, L. Li, Z. Xu, N. Li, Z. Liu, Q. Chen, L.-D. Sun and C.-H. Yan, A Eu<sup>3+</sup>-Eu<sup>2+</sup> ion redox shuttle imparts operational durability to Pb-I perovskite solar cells, *Science*, 2019, **363**, 265.
- 18 W. Lee, M. Jeon, J. Choi, C. Oh, G. Kim, S. Jung, C. Kim, S.-J. Ye and H.-J. Im, Europium-Diethylenetriaminepentaacetic acid loaded radioluminescence liposome nanopatform for effective radioisotope-mediated photodynamic therapy, *ACS Nano*, 2020, **14**, 13004.
- 19 M. Yu, J. Yao, J. Liang, Z. Zeng, B. Cui, X. Zhao, C. Sun, Y. Wang, G. Liu and H. Cui, Development of functionalized abamectin poly(lactic acid) nanoparticles with regulatable adhesion to enhance foliar retention, *RSC Adv.*, 2017, **7**, 11271.

